Cite this article
Nguyen VT, Wu N, Gan Y, Pereira JM and Tang AM (2019)
Long-term thermo-mechanical behaviour of energy piles in clay.
Environmental Geotechnics **XXXX(XXXX)**: 1–XX,
https://doi.org/10.1680/jenge.17.00106

Research Article
Paper 1700106
Received 14/12/2017; Accepted 15/01/2019

Keywords: Q1

Environmental Geotechnics

ice Publishing

Long-term thermo-mechanical behaviour of energy piles in clay

Q2 Q3 Q4

1 **V. T. Nguyen**
Laboratoire Navier – UMR 8205, École des Ponts ParisTech, Ifsttar, CNRS and Université Paris-Est, Marne-la-Vallée, France

2 **N. Wu**
School of Civil Engineering, The University of Sydney, Sydney, Australia

3 **Y. Gan**
School of Civil Engineering, The University of Sydney, Sydney, Australia

4 **J. M. Pereira**
Laboratoire Navier – UMR 8205, École des Ponts ParisTech, Ifsttar, CNRS and Université Paris-Est, Marne-la-Vallée, France

5 **Anh Minh Tang**
Géotechnique (Cermes), Laboratoire Navier – UMR 8205, École des Ponts ParisTech, Ifsttar, CNRS and Université Paris-Est, Marne-la-Vallée, France (corresponding author: anhminh.tang@enpc.fr)
(Orcid:0000-0002-7149-8497)





In engineering practice, energy pile foundations are often designed for the lifetime of the building. Thermal exchange between a pile and the surrounding soil depends on the annual energy needs of the building, as heating mode in winter and cooling mode in summer. Thus, energy pile foundations will undergo a heating–cooling cycle per year. In the present work, an experimental method based on a small-scale pile model installed in saturated clay was used to study the thermo-mechanical behaviour of energy piles under thermal cycles. Thirty cycles were applied (to represent a 30-year period if the daily cycles are neglected) while a constant pile head load was maintained. Four tests were performed corresponding to pile head loads equal to 0, 20, 40 and 60% of pile resistance. The results obtained show an increase in irreversible pile head settlement with the thermal cycles. In order to interpret the experimental results better, the finite-element method is used to simulate the experiments numerically. This allows highlighting the important role of pile thermal contraction/expansion in the pile–soil interaction under thermo-mechanical loading.

Introduction

Q5 Pile foundations are used to erect a structure on an underground with poor load-bearing properties. Energy piles (also called 'heat exchanger piles') are foundation piles that are also used as heat exchangers. A system of heat exchanger pipes is embedded in such piles, allowing exchanges of thermal energy between the ground and the building through a fluid circulating in the pipes. This system combined with a heat pump allows extracting heat from the soil in winter and re-injecting back heat to the soil in summer (Abuel-Naga *et al*., 2015; de Santayana *et al*., 2019). Thus, energy pile foundation is subjected to a heating–cooling cycle per year, which reflects seasonal temperature variations. These annual thermal cycles would then modify the soil–pile interaction from the thermo-mechanical point of view. Despite various studies on the thermo-mechanical behaviour of energy piles, few works have investigated their long-term behaviour. Actually, to deal with this aspect, some studies investigated the mechanical behaviour of energy piles subjected to numerous thermal cycles, which represent the seasonal pile temperature variations (Bidarmaghz *et al*., 2016; Di Donna and Laloui, 2015; Ng *et al*., 2014, 2016; Nguyen *et al*., 2017; Olgun *et al*., 2015; Pasten and Santamarina, 2014; Saggu and Chakraborty, 2015; Suryatriyastuti *et al*., 2014; Vieira and Maranha, 2016). In these studies, numerical methods are usually used and experimental methods are mainly based on physical modelling.

Among the numerical methods, the conventional load transfer method is the simplest one. Suryatriyastuti *et al*. (2014) used this method, combined with additional mechanisms for predicting the degradation behaviour of pile–soil interface under thermal cycles, and investigated the behaviour of free- and restraint-head pile in loose sand. The results show ratcheting of pile head settlement under a constant working load and a decrease in pile head force for the restraint-head pile after 12 thermal cycles. Pasten and Santamarina (2014) developed a modified one-dimensional load transfer model to predict the displacement of pile elements. The results show that the axial force changes mainly in the middle of pile length when the pile works under a heating phase. However, in a cooling phase, the axial force changes are negligible. Moreover, the irreversible settlement of pile reaches a plateau after several thermal cycles.

Besides the load transfer method, the finite-element method is also used to investigate the long-term thermo-mechanical behaviour of energy piles. Saggu and Chakraborty (2015) investigated the behaviour of a floating and end-bearing pile in

loose and dense sand under various thermal cycles by using the finite-element method. The result shows an important settlement of the pile after the first thermal cycle. A similar result can be found in the numerical study of Olgun *et al*. (2015) where pile head displacement and axial stress were investigated under three different climatic conditions for 30 years. After 30 annual thermal cycles, even if the pile was progressively cooled, the axial stress along the pile tended to increase. A decrease in axial stress was observed during heating. This was explained by the difference in the thermal dilation between the pile and the soil during the thermal loading process. Ng *et al*. (2016) studied the horizontal stress change of a soil element close to the pile when the pile is subjected to 50 heating–cooling cycles. The results show that the horizontal stress along the pile depth decreased with thermal cycles. In addition, the irreversible settlement of the pile due to a decrease in the shaft resistance leads to the densification of soil below the pile toe and thus a decrease in the rate of pile's settlement.

Few studies have investigated the long-term thermo-mechanical behaviour of energy pile in clay. Di Donna and Laloui (2015) developed a numerical model for estimating the additional displacement of the pile and the stress–strain state at the soil–pile interface. The result indicates that the upper part of the pile heaves in the heating phase and settles in the cooling phase. The irreversible settlement of the pile is observed in the first cycle, but in the following cycles, the vertical displacement of the pile is almost reversible. A greater plastic strain was obtained within the soil mass at points located close to the soil–pile interface. Vieira and Maranha (2016) investigated the behaviour of a floating pile model in clay soil under different constant static loads and seasonal temperature variations for 5 years using the finite-element method. The considered soil is saturated and normally consolidated. The results indicate that when the pile works with a high factor of safety, its displacement is reversible during the thermal cycles. However, a low factor of safety induces an increase in axial stresses, while the rate of irreversible settlement reduces with the number of cycles.

Aside from the numerical studies mentioned earlier, few experimental studies have been performed to investigate the long-term behaviour of energy piles in clay. Ng *et al*. (2014) used centrifuge modelling to study the thermo-mechanical behaviour of energy piles constructed in lightly and heavily overconsolidated clay under five thermal cycles. The results show that the most irreversible settlement of pile was observed in the first thermal cycle, and then in the following cycles, the settlement increases at a lower rate. After five cycles, the cumulative settlement was about 3·8%·D (D being the pile diameter) for a pile in the lightly overconsolidated clay and 2·1%·D in the case of heavily overconsolidated clay.

In the present work, the long-term thermo-mechanical behaviour of an energy pile in clay is investigated by both physical and numerical modelling. First, a small-scale pile model installed in saturated clay was used. Thirty thermal cycles were applied while the pile head load was maintained constant at 0, 20, 40 and 60% of pile bearing capacity. Second, the finite-element method is used to simulate numerically the experiments. The results of the two methods are finally analysed simultaneously to identify better the main mechanisms controlling the thermo-mechanical behaviour of an energy pile under several thermal cycles. The novelty of the work consists in integrating results of a small-scale pile model (physical modelling) with those obtained by numerical modelling (finite-element numerical model). As mentioned earlier, few (and very recent) works can be found in the literature dealing with the long-term mechanical effect on energy geostructures (energy piles, in the present case) under thermal cycles.

Physical modelling

The pile model is made of an aluminium tube with internal and external diameters of 18 and 20 mm, respectively. The length of the tube is 800 mm, and it is sealed at the bottom. Its external surface was coated with sand to imitate the roughness of a full-scale bored pile; 600 mm of the pile was embedded in saturated clay (see Figure 1).

The pile temperature is controlled by a metallic U-tube inserted inside it and connected to a cryostat. A temperature sensor (accuracy equals ±0·01°C) is embedded inside the pile, at 300 mm depth, to monitor its temperature during the experiments. The axial load applied to the pile head is controlled by a dead weight

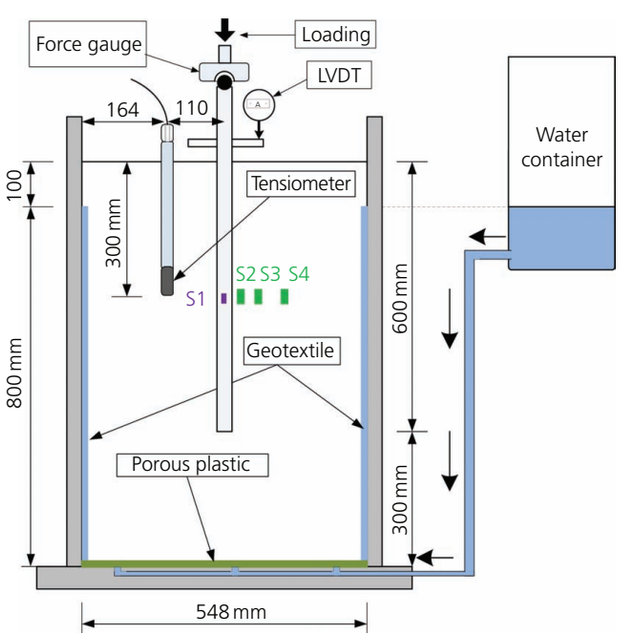

S1 Temperature transducer inside the pile
S2–S4 Temperature transducer distributed in soil

Figure 1. Experiment set-up. LVDT, linear variable differential transformer

(more details on a similar set-up can be found in the paper of Yavari *et al*. (2014)) and measured by a force sensor. The pile head displacement is measured by a displacement sensor (linear variable differential transformer) with an accuracy of ±0·001 mm. The temperature in soil is measured by three sensors embedded at 300 mm depth and 20, 40 and 80 mm from the pile axis.

Speswhite kaolin clay was used in this study. It has a clay fraction of 30%, a liquid limit of 57%, a plastic limit of 33% and a particle density of 2·60 Mg/m^3. Clay powder was mixed with water by using a soil mixer to achieve a water content of 29%. It is then stored in a sealed box for 1 month for moisture homogenisation. Compaction was performed, into a layer of 50 mm thickness, using an electrical vibratory hammer. The soil mass used for the compaction of each layer was controlled to obtain a dry density of 1·45 Mg/m^3 (degree of saturation equals 95% and void ratio equals 0·79). After the compaction of the first six layers, the model pile was installed in place and the remaining soil layers were completed. At the vicinity of the pile model, a small metal hammer was used to avoid damaging the pile.

To control the quality of the compaction procedure, soil samples (20 mm dia.) were cored from the compacted soil mass for the determination of dry density and water content. The created hole was refilled afterwards prior to the test with energy pile. Results show that the dry density and the water content are relatively uniform with depth and they are close to the target values (Figure 2).

In the work of Yavari *et al*. (2016a), resaturating a similar soil mass from the bottom took several months. In the present work, to speed up this phase, a porous plastic plate was installed at the bottom of the soil container and a thin geotextile layer was installed between the container internal surface and the soil mass (see Figure 1). Thus, water from the container can easily flow through the small holes at the bottom of the soil container and diffuse into the soil mass through the porous plastic plate and the surrounding geotextile. The water level in the water container was kept 100 mm below the soil surface to avoid water overflow on the soil surface. During the saturation, a tensiometer (T8, UMS, 2008) was used to control the soil suction at 300 mm depth and 110 mm away from the pile's axis (see Figure 1). The result in Figure 3 shows that after 18 d of saturation, the soil suction at the tensiometer position is very close to zero. The tensiometer was then removed, and the resulting hole was refilled to avoid its influence on the thermo-mechanical behaviour of the pile. The saturation process was kept for 45 d in total to ensure the full saturation of the soil mass. In should be noted that during the saturation, the soil container was covered on its surface to avoid water evaporation and heat exchange. Moreover, the saturation system was maintained during the subsequent thermo-mechanical experiment to ensure that the soil is always saturated.

Before conducting the experiment, the temperature of the soil and pile was kept at 20°C for 1 week. This temperature was close to the room temperature during that period. After the saturation process, the pile was initially subjected to a mechanical load (test A1) to determine its ultimate bearing capacity. A series of load steps was applied to the pile head with increments of 50 N, each

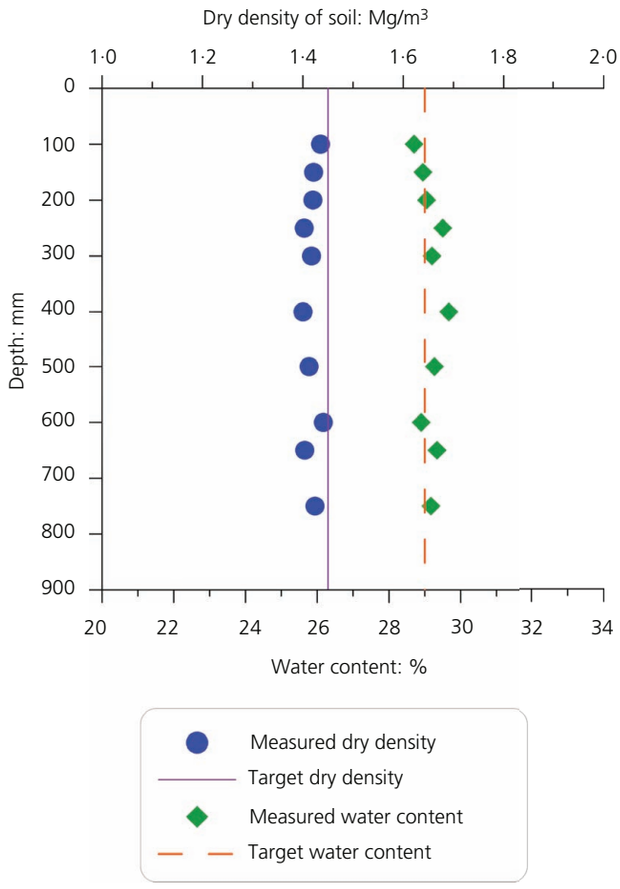

Figure 2. Dry density and water content of compacted soil

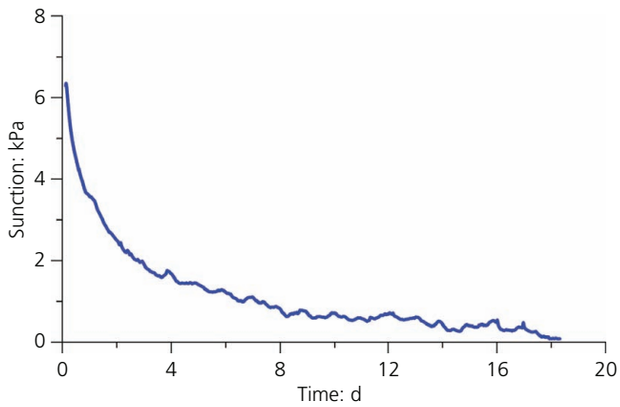

Figure 3. Evolution of soil suction during the saturation process (measured by a tensiometer)

loading step being maintained for 1 h, following the French standard (Afnor, 1999). The results, shown in Figure 4, are similar to those obtained by Yavari *et al*. (2016a). This confirms the repeatability of the applied experimental procedure.

In test A1, the pile was loaded up to 500 N, which corresponds also to the pile's bearing capacity. After this test, the pile head load was removed. In test A2, 30 thermal cycles were performed while no load was applied to the pile head. Afterwards, the pile head was loaded up to 20% of the pile's capacity prior to the application of 30 thermal cycles (test A3 shown in Figure 4). At the end of these cycles, the pile head load was removed and then a load corresponding to 40% of the pile's capacity was applied. Thirty thermal cycles were then performed under this load (test A4). A similar procedure was applied for test A5 corresponding to 60% of pile's capacity. This procedure is similar to that applied by Yavari *et al*. (2016a) where only one thermal cycle was applied per load step. All the five tests were performed on the same soil mass. The mechanical test (A1) was performed at first to identify the pile's capacity. This allowed better defining the programme for the subsequent thermo-mechanical tests (A2–A5). Yavari *et al*. (2016a) found that loading the pile to its ultimate bearing capacity and then unloading it did not modify its behaviour during the subsequent tests.

For each thermal cycle, the pile temperature is increased and then decreased with a variation of ±1°C around the initial value (shown as the thermal sensor S1 in Figure 5). This range is much smaller than the temperature variation in the energy piles, which can reach up to ±20°C (Di Donna and Laloui, 2015; Olgun *et al*., 2015). Actually, in this small-scale model, the dimension of the pile is 20 times smaller than a full-scale pile 0·4 m dia. and 12 m long. As a consequence, the strain related to the mechanical load is 20 times smaller than that at the full scale (Laloui *et al*., 2006; Ng *et al*., 2014). For this reason, the temperature variation was reduced 20 times in order to have a thermal strain of the pile 20 times smaller than that at the full scale. Each thermal cycle is completed within 24 h, which started with a heating period of 4 h, and followed by a cooling period of 4 h; finally, the remaining time corresponded to active heating to return to the initial temperature.

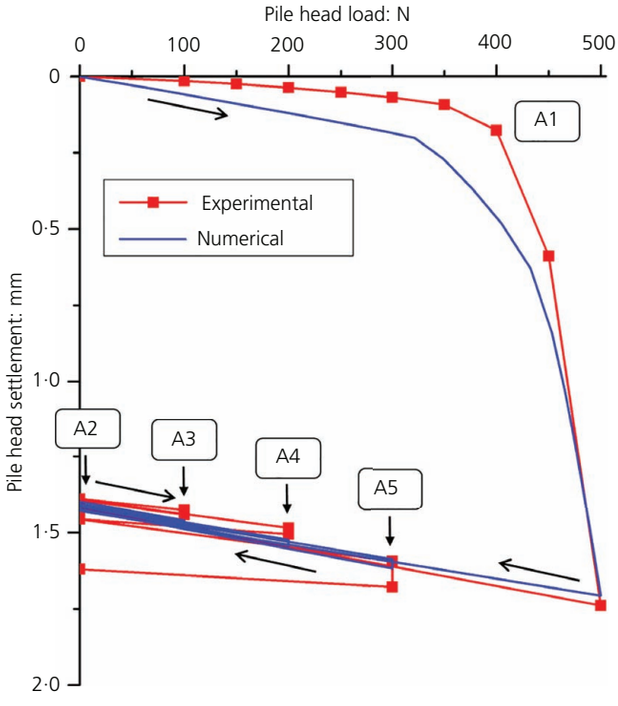

Figure 4. Pile head load–displacement curve: A1 is a purely mechanical test; A2, A3, A4 and A5 are thermo-mechanical tests

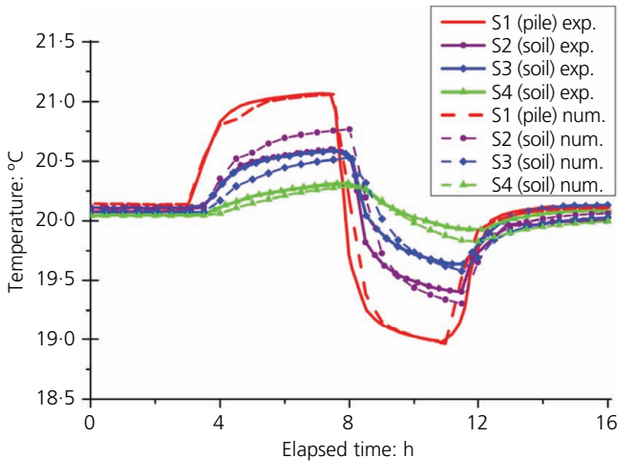

Figure 5. Temperature of pile and surrounding soil during one thermal cycle

Numerical modelling

Axisymmetric finite-element model

The finite-element analysis (FEA) was performed by using the commercial FEA software Abaqus V6.16. To model the physical experiment, a two-dimensional axisymmetric model is established (as shown in Figure 6), and fully coupled four-node temperature–pore pressure–displacement element (CAX4PT) and four-node bilinear displacement–temperature element (CAX4T) are used for the regions of soil and pile, respectively. Soil is assumed fully saturated throughout the loading cycles. and the top 100 mm capillary zone in physical model is ignored. Pore pressure at top surface of soil is opened to air, but no heat flow escapes from top surface. A circular hollow section aluminium pile is modelled by a solid pile with an equivalent mass density. The soil is modelled by the modified Cam-clay model, and the pile is described by a linear-elasticity model. For contact properties, the friction coefficient at the soil–pile interface is assumed to be $\tan\phi$, where ϕ is the soil friction angle. Note that a relatively large thermal conductance is chosen at pile–soil interface to reduce the interfacial thermal contact resistance. A lateral pressure coefficient is assumed based on the Meyerhof correlation, $K_0 = (1 -$

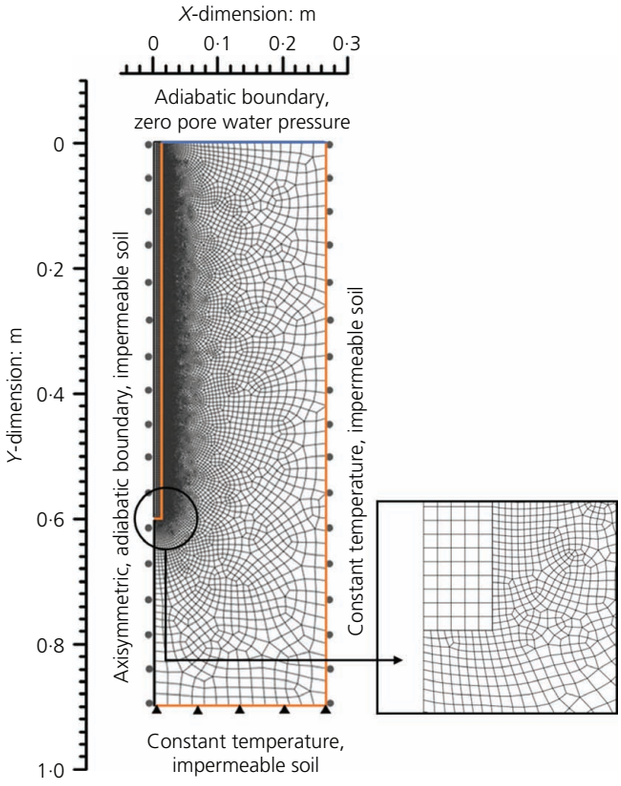

Figure 6. Geometry and boundary conditions of the numerical model

Table 1. Parameters of pile and soil in numerical modelling

Parameter	Pile (CHS aluminium)	Clay (Speswhite kaolin clay)
Constitutive model	Linear-elastic	Modified Cam-clay
Dry density: Mg/m^3	1·32	1·45
Volumetric weight at saturated state: kN/m^3	N/A	18·53
Young's modulus E: kPa	1·3 × 10^7	N/A
Poisson's ratio ν[a]	0·33	0·25
Slope of critical state line M[a]	N/A	0·98
Slope of virgin consolidation line λ[a]	N/A	0·14
Slope of swelling line κ[a]	N/A	0·012
Initial void ratio e_0[a]	N/A	1·6
Void ratio after compaction e_1	N/A	0·79
Friction angle ϕ:[a] °	N/A	25
Permeability k:[a] m/s	N/A	1 × 10^{-8}
Thermal expansion: /°C	2·3 × 10^{-5}	1 × 10^{-6}
Thermal conductivity: W/(m °C)	237	1·5
Specific heat capacity: J/(kg °C)	9 × 10^2	1·269 × 10^3

[a] Soil properties are adopted from the paper of Lv *et al.* (2017)

Table 2. Other relevant parameters in numerical modelling

Volumetric weight of water: kN/m^3	9·81
Friction coefficient tan ϕ	0·47
Interfacial thermal conductance: W/(°C m^2)	500
Lateral earth coefficient, K_0	8

Q7 $\sin\phi)\mathrm{OCR}^{0·5}$, by taking the pressure at two-thirds the depth of the pile for averaging pressure along the pile to estimate K_0, and OCR is approximately 160. The calculation of OCR is based on the ratio of the historical maximum pressure to the current experienced pressure. Q8 The former is calculated based on the Cam-clay model parameters from Lv *et al.* (2017) for the normal compression line – that is, 560 kPa with the experimentally measured void ratio of 0·79. As a result, $K_0 = 8$ is adopted for the numerical simulation, and it is within a reasonable range since preparation of physical model involves a precompaction process. All parameters in the simulation are summarised in Tables 1 and 2, and the constitutive parameters of soil can be referred to paper of Lv *et al.* (2017). The initial temperature for the entire numerical model is assumed 20°C as the case of the physical model. Bottom and side boundaries are set as a constant temperature of 20°C. Deformation of soil is fully fixed at the bottom and only horizontally fixed at the side, while the top surface is free to deform. Finite sliding formulation is used at the soil–pile interface.

Temperature variation with time in the physical experiment is deemed to be an input parameter for investigating settlement occurring under the cyclic thermal loading condition. To simplify the model, the entire pile is going to experience temperature variation uniformly instead of the water circulation process in the experiment. Thirty heating and cooling cycles are applied in every thermal loading stage after the given mechanical load. One complete thermal cycle includes four different thermal phases, initial, heating, cooling and reheating, which will induce settlement fluctuation.

Mesh sensitivity study

Five different mesh convergence analyses were performed to study mesh dependency of the numerical model. For the pile, uniform 1, 2 and 3 mm seed sizes are applied in the pile region with an unchanged 1 mm mesh size at the soil side of the soil–pile interface to find the appropriate pile mesh size. It is found that a 2 mm mesh size for the pile was sufficient, and then, mesh sizes of 1, 1·5 and 2 mm are applied into the soil side of the soil–pile interface region, which enables in total five different types of mesh size combinations. At the far end, bottom and side of the soil, the mesh seed size was set to a fixed 20 mm value for all simulations. Here only the purely mechanical loading condition, A1, was considered for this mesh convergence study, which was similar to Wehnert and Vermeer's (2004) work. In Q10 Figure 7, load–settlement curves for different mesh size combinations are given. The mesh 'Pile 2 mm, soil 1 mm' is selected since it is above the threshold (i.e. 'Pile 2 mm, soil 1·5 mm') compared with the experimental data for the pure mechanical loading. This finer mesh provides a better confidence for the results from later thermo-mechanical analyses, while only slightly increasing the demand on computational resources.

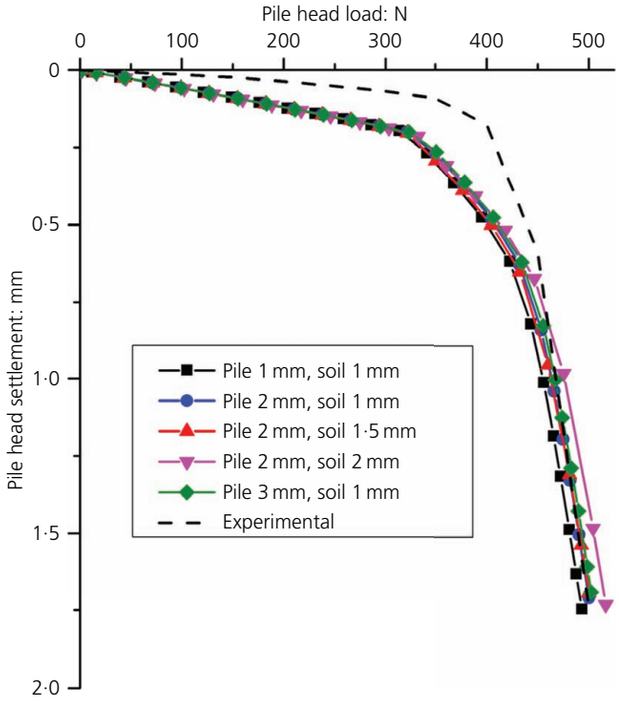

Figure 7. Mesh dependency results (A1)

Results

Mechanical behaviour of the pile

The experimental result of test A1 is shown in Figure 4. This load–settlement curve is based on the settlement value at the end of each load step. After loading to 500 N, the pile is unloaded and the irreversible settlement of the pile head is about 1·42 mm. The relationship between the axial load and the pile head settlement during the loading is almost linear when the axial load is smaller than 350 N. For an axial load higher than this value, the pile head settlement increases significantly with increase in axial load.

The numerical result gives a similar behaviour of the pile by using the parameters of the pile and soil shown in Tables 1 and 2. Analysis on the plastic points shows that during the loading path, when the axial load is lower than 350 N, only few plastic points can be observed at the pile toe. Interfacial friction is approaching the maximum shear stress. Loading above this value induces development of plastic zones, and this phenomenon can be observed as the quick increase in pile head settlement.

Thermo-mechanical behaviour of the pile

In this section, the results of the tests from A2 to A5 are presented. Figure 8 shows the temperature distribution corresponding to four phases of one thermal cycle: initial, heating, cooling and reheating. These results confirm that the heat transfer between the pile and the surrounding soil is mainly radial along the pile. The temperature measured at 300 mm depth (in the middle of the pile) should be then representative for studying the heat transfer in this study.

Actually, Figure 5 presents the temperatures measured at different locations at 300 m depth during one thermal cycle. These measurements evidence that the soil temperature increases when the pile is heated and decreases when the pile is cooled. The effect of pile heating/cooling is more significant for sensors located closer to the pile. The numerical results obtained in the soil are in good agreement with the experimental ones. This agreement confirms that the thermal parameters and the heat transfer mechanisms (heat conduction) used in the numerical model are appropriate. Note that the thermal parameters have been determined separately in laboratory by a thermal probe.

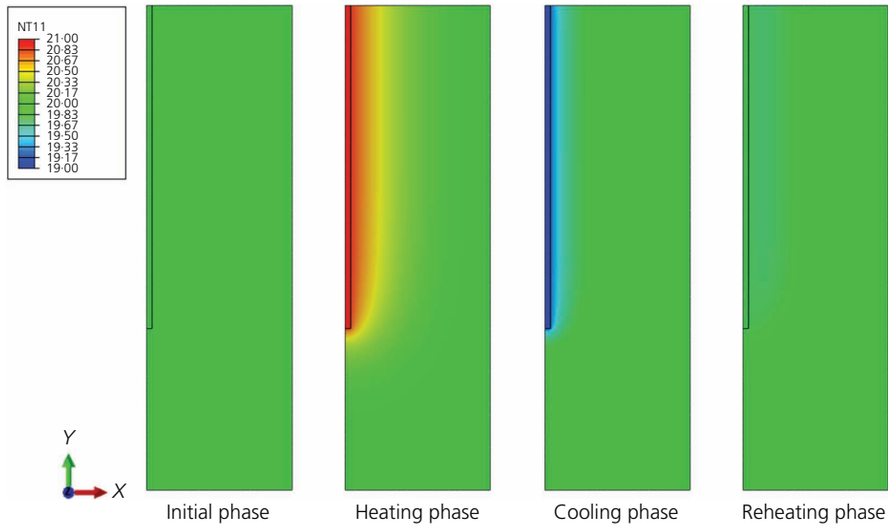

Figure 8. Temperature distribution during one thermal cycle obtained from numerical modelling

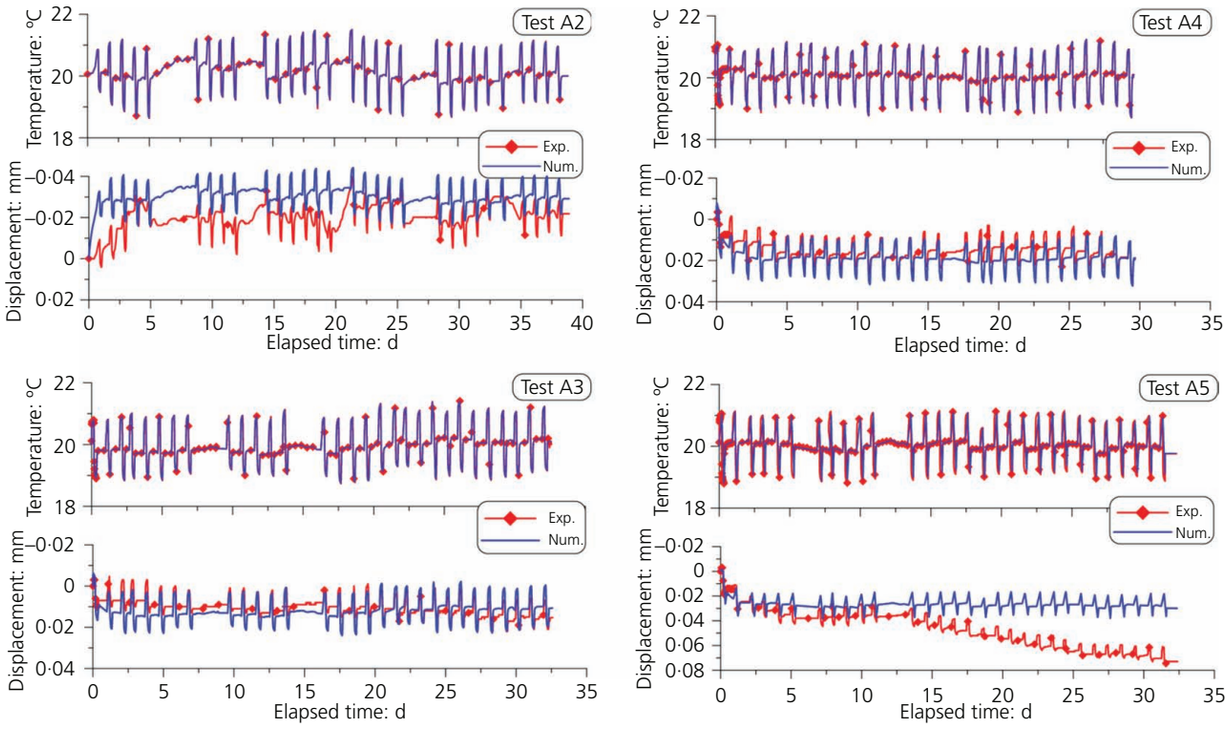

Figure 9. Temperature and pile head displacement plotted against elapsed time (A2–A5)

Figure 9 shows the results of temperature and displacement of the pile over the 30 thermal cycles under different loads. It can be seen that the target temperature (20°C–21°C–19°C–20°C) in each thermal cycle could not be strictly respected during the first test (A2). This is related to the variation in temperature in the room. For this reason, in the subsequent tests (A3, A4 and A5), the thermal isolation of the tube connecting the cryostat and the pile was improved, which allowed reducing significantly the influence of room temperature on the pile temperature. In Figure 9, the pile head settlement of each test is set to zero at the beginning of the thermal cycles. The results show generally a pile head heave during heating and settlement during cooling. However, the relation between the pile head displacement and the pile temperature is not strictly reversible. Note that the temperature was controlled manually, and for some cycles corresponding to weekend periods, the active heating phase took longer than 2 d. Nevertheless, it seems that these longer phases do not influence significantly the results.

In the numerical model, the pile temperature measured in the experiment is imposed to the whole pile to simulate the thermal cycles under constant pile head load. The pile head settlement obtained by the simulation is also shown in Figure 9. The numerical results show equally a pile head heave during heating and settlement during cooling. More details on pile head displacement during each thermal cycle and the irreversible pile head displacement are shown in Figures 10 and 11.

To analyse better the pile head displacement during each thermal cycle, in Figure 10, it is plotted against pile temperature for the first and the last cycles only. The free-expansion curve, obtained with the assumption of a pile restrained at its toe, is also plotted. In each thermal cycle, heating induces pile head heave and cooling induces pile head settlement. For A3, A4 and A5 (under constant head load), the first thermal cycle induces a significant irreversible settlement. For the case of test A2 where no head load was applied, the behaviour during the first thermal cycle is quite reversible. For the last thermal cycle, a reversible behaviour can be observed for all the tests. Moreover, it can be noted that the slope of the pile head displacement against temperature change during the cooling phase is slightly smaller than that of the free-expansion curve.

The results obtained by the numerical simulation are generally in agreement with the experimental ones. Actually, the behaviour obtained during the last thermal cycles is strictly reversible and the first thermal cycle in tests A3, A4 and A5 (under constant pile head load) induces significant reversible settlement. Only the behaviour of the first cycle of test A2 (without pile head load) shows a difference. In the numerical model, an irreversible pile head heave was obtained after the first thermal cycle.

The irreversible pile head displacement is plotted against the number of cycles in Figure 11. For a better comparison with full-scale experiments, it is also normalised with the pile diameter. For test A2,

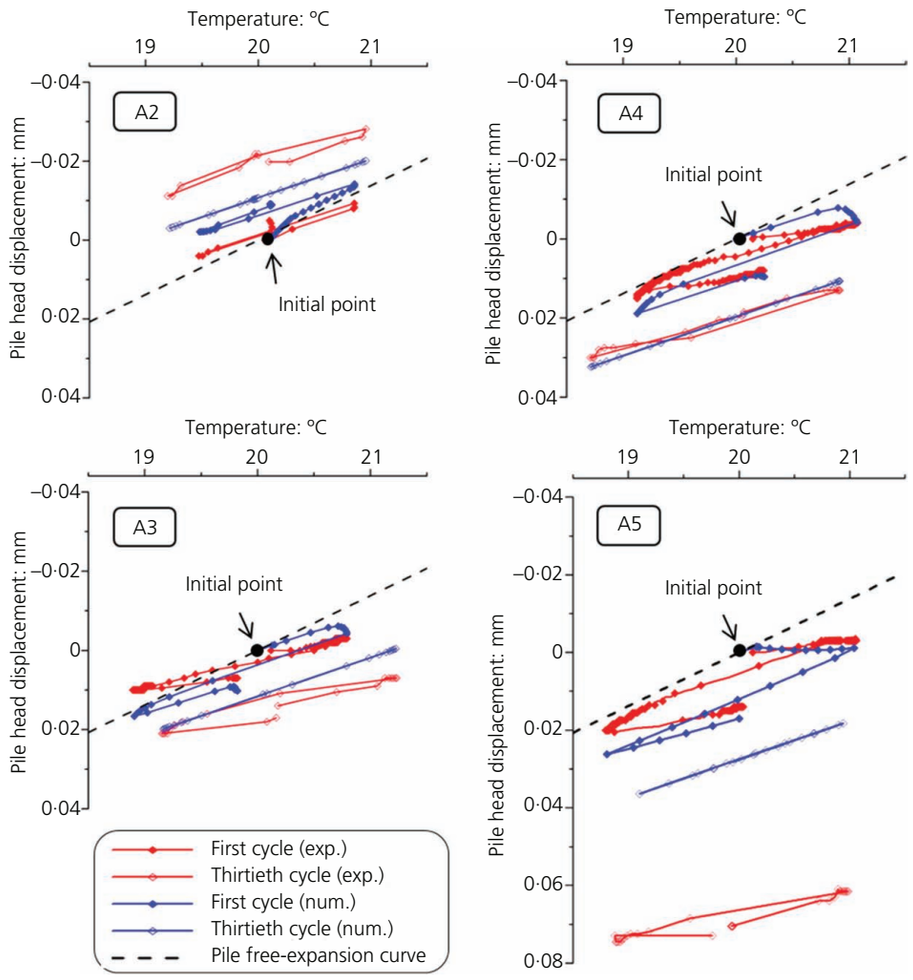

Figure 10. Pile head settlement plotted against pile temperature during the first and the thirtieth cycles

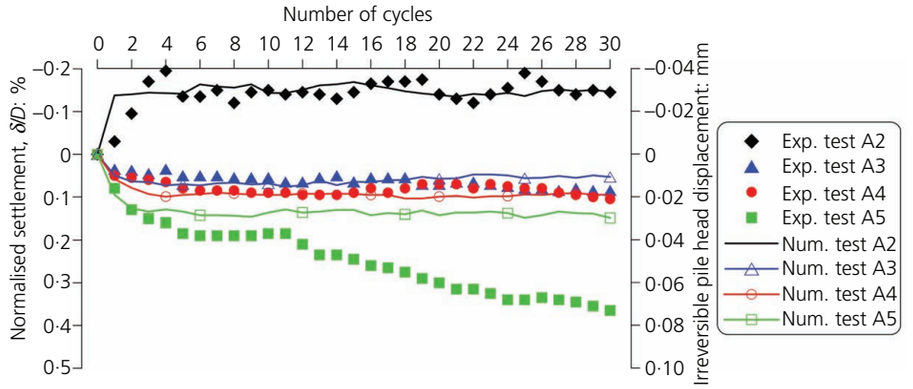

Figure 11. Irreversible pile head displacement plotted against number of thermal cycles

the first cycle induces pile head heave up to 0·15% of the pile diameter with the numerical model. Afterwards, the pile behaviour remains reversible during thermal cycles. However, with the physical model, the first cycle induces only a very small pile heave (0·03% of the pile diameter). However, pile heave continues to increase during the subsequent cycles and reaches 0·20% of pile diameter after four cycles. For tests A3 and A4, the first thermal cycles induce significant irreversible settlement. This later becomes negligible for the subsequent cycles. The behaviour of the pile in test A5 is also similar to that in tests A3 and A4. However, after the tenth cycle, the irreversible settlement increases continuously with the increase in the number of cycles. Furthermore, it can be noted that the irreversible settlement depends on the pile head load; the higher the pile head load, the higher the irreversible settlement. For test A5, the sudden increase in irreversible settlement from the tenth cycle should be related to some technical problems. The possible causes of problems occurred could be tilting of the pile at high cumulative settlement, failure of soil around the pile toe or other physico-chemical phenomena that occur in soil after a long period (several months).

The results obtained by the numerical simulation are generally in good agreement with the experimental ones. The only difference is related to test A5, where the pile head irreversible displacement remains constant event after the tenth cycle in the numerical simulation.

The long-term performance of the pile is further illustrated according to the numerical results. The vertical displacement of pile length in the heating phase (H), cooling phase (C) and reheating phase (R) are plotted in Figure 12. The first, second, 20th and 30th thermal cycles are selected here because simulation results show that the majority of irreversible settlement happens within the first three cycles and is relatively stable in the rest of thermal cycles. Note that the vertical displacement of the pile is assumed zero at the beginning of the first cycle in order to be consistent with Figure 11. It is obvious that heating and cooling the pile cause displacement distribution to be mirror-reflecting each other and the vertical displacement remains constant along the pile length in the reheating phase. The time evolution of the displacement profile is stabilised over a few cycles with a null point at about 430 mm beneath the top surface.

The total vertical stress along the pile length under different thermal cycles obtained from the numerical simulation is presented in Figure 13. Only the results obtained from the first and the last cycles are presented for clarity. Generally, heating the

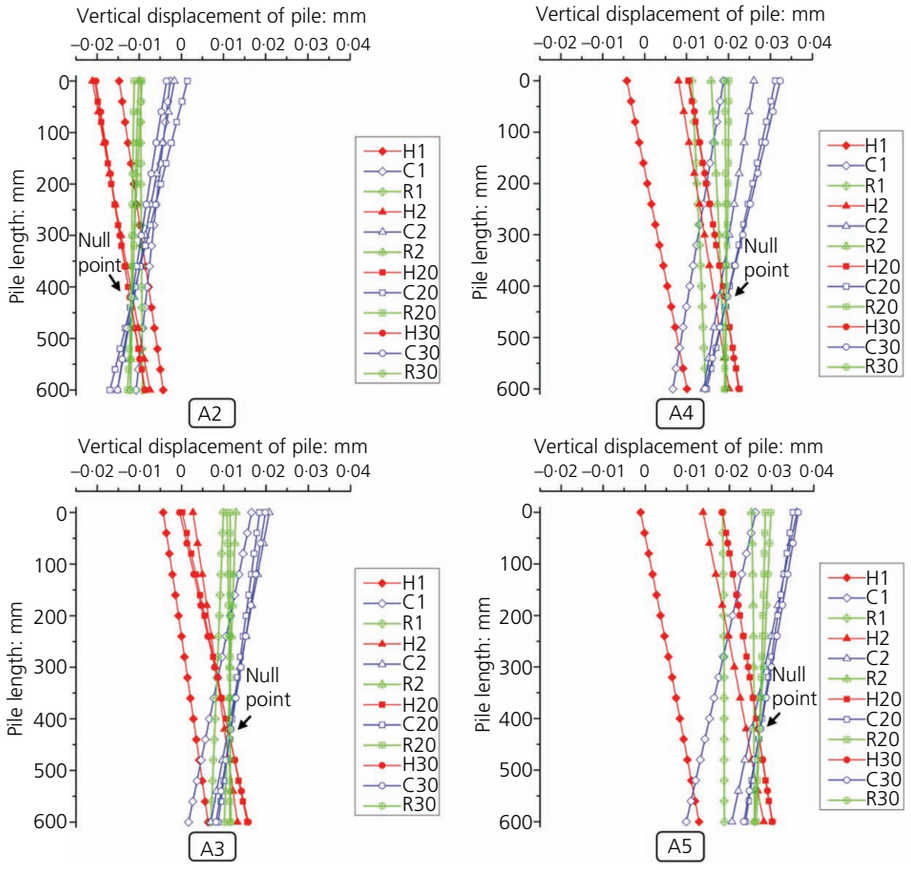

Figure 12. Vertical displacement along the pile length (numerical results)

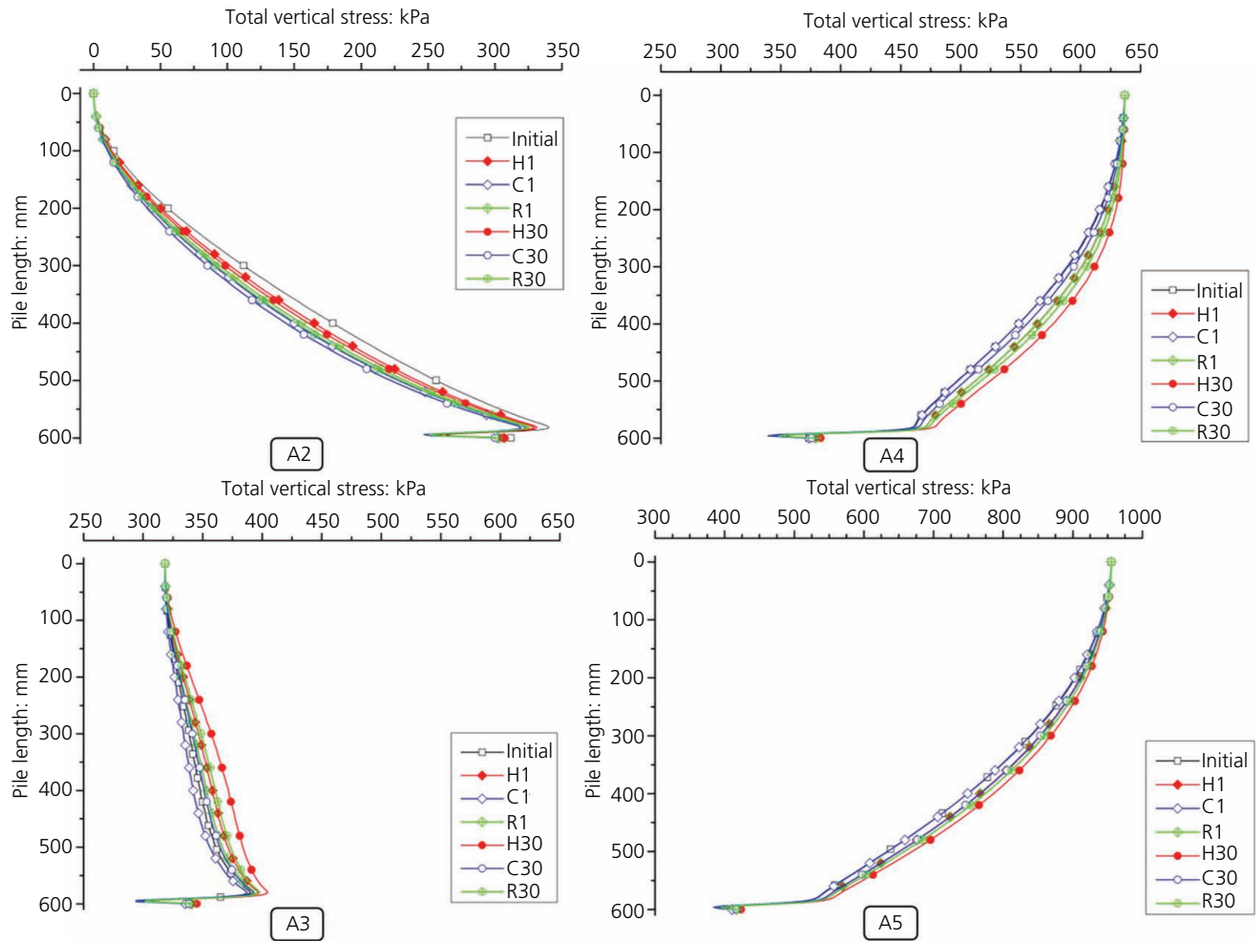

Figure 13. Thermal effect on the total vertical stress along the pile length (numerical results)

pile induces a slight increase in vertical stress and cooling causes a decrease in vertical stress distribution along the pile length. The behaviour obtained during the first cycle of test A2 is slightly different; heating induces a decrease in vertical stress and cooling decreases it again. In addition, the vertical stress is observed to increase slightly from the first to the last thermal cycle in all heating, cooling and reheating phases.

Discussion

In the mechanical test paths (test A1), the material parameters for the numerical simulation are adopted from the paper of Lv *et al.* (2017). From the results, it is obvious that the estimated bearing capacity is in agreement with the experimental results (Figure 4). A carefully estimated lateral stress coefficient (K_0) is important to consider the compaction process in physical model.

In test A2, the upward displacement of the pile (as shown in Figure 9) during heating–cooling cycles, observed on both physical and numerical models, can be explained by the stress state shown in Figure 13. Actually, test A2 starts after the mechanical unloading path of test A1. At the end of the unloading path, the pile is still subjected to compressive stress (up to 300 kPa at its toe). Thermal cycles in test A2 induce thermal dilation/contraction of the pile. This movement would release this compressive stress and heave the pile. The results shown in Figure 13 evidence this stress release after thermal cycles.

In the subsequent tests (A3, A4 and A5), irreversible settlement was observed during the first thermal cycles. These results are in agreement with those observed by Ng *et al.* (2014) (using centrifuge modelling) and Vieira and Maranha (2016) by using the finite element method. However, only five thermal cycles were investigated in these works. Actually, the axial stress profiles plotted in Figure 13 show that these thermal cycles increase the axial stress along the pile. That means the thermal dilation/contraction of the pile facilitates the transmission of the axial pile head load to the pile toe. In the present works, both numerical and physical models show that the pile settlement becomes reversible under thermal cycles at high number of cycles (except for test A5).

The numerical model shows a behaviour similar to that obtained by the physical model; the pile settlement progressively achieves a stable state due to the densification process in each thermal cycle. In particular, the first thermal cycle shows good agreement with the experimental result (Figure 10). The explanation of why numerical simulation is able to predict progressive settlement owes to the use of the modified Cam-clay model as the constitutive model for soil. The Cam-clay criterion follows the poro-plasticity rule that could more effectively simulate densification process during thermal cyclic loads, whereas the Mohr–Coulomb model may not well describe such soil behaviour (Yavari *et al*., 2014). Therefore, the present numerical prediction of long-term thermal cyclic settlement of an energy pile is able to predict experimental data with relatively good agreement.

The results of Figure 10 show that the slope of the plot of the pile head displacement against temperature change during the cooling phase is slightly smaller than that of the free-expansion curve. Actually, similar tests on dry sand have shown that this slope is similar to the free-expansion curve (Kalantidou *et al*., 2012; Yavari *et al*., 2014). The behaviour observed in the present work can be explained by the results shown in Figure 12. Actually, the null point is not located at the pile toe but at 400–450 mm depth. For this reason, the pile head displacement does not correspond to the free expansion of the whole pile length.

In the present work, the numerical model was able to reproduce correctly the thermo-mechanical behaviour of a small-scale energy pile under several thermal cycles. Note that the range of the temperature variation in the physical model was limited to ±1°C. This value is much smaller than full-scale application (up to ±20°C) in order to respect the scale effect. Within this limited range of temperature variation, the soil parameters can be assumed to be independent of temperature. However, for a higher temperature variation, the temperature change can slightly modify the soil properties (Ghorbani *et al*., 2019; Hong *et al*., 2016; Jacinto and Ledesma, 2017; Tang *et al*., 2008; Vega and McCartney, 2015; Yavari *et al*., 2016b). The use of the present numerical model to predict the behaviour of real-scale energy foundations should consider this aspect.

Results obtained in the present study would be helpful for studies on various types of thermo-active geostructures (Angelotti and Sterpi, 2019; Baralis *et al*., 2019; Hoyos *et al*., 2015; Narsilio *et al*., 2017; Sanchez *et al*., 2017).

Conclusions

The long-term thermo-mechanical behaviour of an energy pile is investigated in the present work by using a small-scale model pile (physical modelling) and the finite-element method (numerical modelling). The following conclusions can be drawn.

- Thermal cycles applied to the pile under a constant pile head load induce stress redistribution inside the pile. This can induce irreversible pile heave in the case without a pile head load and irreversible pile settlement in the case with pile head load.
- The irreversible pile head settlement/heave is more important within the first thermal cycles; it becomes negligible at high number of cycles.
- The main mechanism that controls the soil–pile interaction during thermal cycles under constant pile head load is the pile thermal contraction/dilation. The numerical model can capture correctly the experimental result without considering the temperature effect on soil parameters.

The preliminary results shown in this paper could warrant future numerical studies for the serviceability design of geothermal energy piles.

Acknowledgements

Dr Gan acknowledges the financial support of Labex MMCD for his stay at Laboratoire Navier. Labex MMCD benefits from a French government grant managed by ANR within the frame of the national programme Investments for the Future ANR-11-LABX-022-01.

REFERENCES

Abuel-Naga H, Raouf MIN, Raouf AMI and Nasser AG (2015) Energy piles: current state of knowledge and design challenges. *Environmental Geotechnics* **2(4)**: 195–210.

Afnor (Association Française de Normalisation) (1999) NF P 94-150-1: Essai statique de pieu isolé sous un effort axial. Afnor, Paris, France (in French).

Angelotti A and Sterpi D (2019) On the performance of energy walls by monitoring assessment and numerical modelling: a case in Italy. *Environmental Geotechnics*, https://doi.org/10.1680/jenge.18.00037.

Baralis M, Barla M, Bogusz W *et al.* (2019) Geothermal potential of the NE extension Warsaw (Poland) metro tunnels. *Environmental Geotechnics*, https://doi.org/10.1680/jenge.18.00042.

Bidarmaghz A, Francisca FM, Makasis N and Narsilio GA (2016) Geothermal energy in loess. *Environmental Geotechnics* **3(4)**: 225–236, https://doi.org/10.1680/jenge.15.00025.

de Santayana FP, de Santiago C, de Groot M *et al.* (2019) Effect of thermal loads on pre-cast concrete thermopile in Valencia, Spain. *Environmental Geotechnics*, https://doi.org/10.1680/jenge.17.00103.

Di Donna A and Laloui L (2015) Numerical analysis of the geotechnical behaviour of energy piles. *International Journal for Numerical and Analytical Methods in Geomechanics* **39(8)**: 861–888, https://doi.org/10.1002/nag.2341.

Ghorbani J, El-Zein A and Airey DW (2019) Thermo-elasto-plastic analysis of geosynthetic clay liners exposed to thermal dehydration. *Environmental Geotechnics*, https://doi.org/10.1680/jenge.17.00035.

Hong PY, Pereira JM, Cui YJ and Tang AM (2016) A two-surface thermomechanical model for saturated clays. *International Journal for Numerical and Analytical Methods in Geomechanics* **40(7)**: 1059–1080, https://doi.org/10.1002/nag.2474.

Hoyos LR, DeJong JT, McCartney JS *et al.* (2015) Environmental geotechnics in the US region: a brief overview. *Environmental Geotechnics* **2(6)**: 319325, https://doi.org/10.1680/envgeo.14.00024.

Jacinto AC and Ledesma A (2017) Thermo-hydro-mechanical analysis of a full-scale heating test. *Environmental Geotechnics* **4(2)**: 123–134, https://doi.org/10.1680/jenge.15.00049.

Kalantidou A, Tang AM and Pereira JM (2012) Preliminary study on the mechanical behaviour of heat exchanger pile in physical model. *Géotechnique* **62(1)**: 1047–1051, https://doi.org/10.1680/geot.11.T.013.

Laloui L, Nuth M and Vulliet L (2006) Experimental and numerical investigations of the behaviour of a heat exchanger pile. *International*

Journal for Numerical and Analytical Methods in Geomechanics **30(8)**: 763–781, https://doi.org/10.1002/nag.499.

Lv YR, Ng CWW, Lam SY, Liu HL and Ma LJ (2017) Geometric effects on piles in consolidating ground: centrifuge and numerical modeling. *Journal of Geotechnical and Geoenvironmental Engineering* **143(9)**: 04017040.

Narsilio GA, Sanchez M, Alvarellos J and Guimaraes L (2017) Editorial: XV Pan-American Conference: selected papers on energy geotechnics. *Environmental Geotechnics* **4(2)**: 67–69, https://doi.org/10.1680/jenge.2017.4.2.67.

Ng CWW, Shi C, Gunawan A and Laloui L (2014) Centrifuge modelling of energy piles subjected to heating and cooling cycles in clay. *Géotechnique Letters* **4(4)**: 310–316, https://doi.org/10.1680/geolett.14.00063.

Ng CWW, Ma QJ and Gunawan A (2016) Horizontal stress change of energy piles subjected to thermal cycles in sand. *Computers and Geotechnics* **78(2016)**: 54–61, https://doi.org/10.1016/j.compgeo.2016.05.003.

Nguyen VT, Tang AM and Pereira JM (2017) Long-term thermo-mechanical behavior of energy pile in dry sand. *Acta Geotechnica* **12(4)**: 729–737.

Olgun CG, Ozudogru TY, Abdelaziz SL and Senol A (2015) Long-term performance of heat exchanger piles. *Acta Geotechnica* **10(5)**: 553–569, https://doi.org/10.1007/s11440-014-0334-z.

Pasten C and Santamarina JC (2014) Thermally induced long-term displacement of thermoactive piles. *Journal of Geotechnical and Geoenvironmental Engineering* **140(5)**: 6014003, https://doi.org/10.1061/(ASCE)GT.1943-5606.0001092.

Q14 Pasten C, Shin H and Santamarina JC (2013) Long-term foundation response to repetitive loading. *Journal of Geotechnical and Geoenvironmental Engineering* **140(4)**: 4013036, https://doi.org/10.1061/(ASCE)GT.1943-5606.0001052.

Saggu R and Chakraborty T (2015) Cyclic thermo-mechanical analysis of energy piles in sand. *Geotechnical and Geological Engineering* **33(2)**: 321–342, https://doi.org/10.1007/s10706-014-9798-8.

Sanchez M, Falcao F, Mack M *et al.* (2017) Salient comments from an expert panel on energy geotechnics. *Environmental Geotechnics* **4(2)**: 135–142, https://doi.org/10.1680/jenge.16.00008.

Suryatriyastuti ME, Mroueh H and Burlon S (2014) A load transfer approach for studying the cyclic behavior of thermo-active piles. *Computers and Geotechnics* **55**: 378–391, https://doi.org/10.1016/j.compgeo.2013.09.021.

Tang AM, Cui YJ and Barnel N (2008) Thermo-mechanical behaviour of compacted swelling clay. *Géotechnique* **58(1)**: 45–54, https://doi.org/10.1680/geot.2008.58.1.45.

Vega A and McCartney JS (2015) Cyclic heating effects on thermal volume change of silt. *Environmental Geotechnics* **2(5)**: 257–268, https://doi.org/10.1680/envgeo.13.00022.

Vieira A and Maranha JR (2016) Thermoplastic analysis of a thermoactive pile in a normally consolidated clay. *International Journal of Geomechanics* **17(1)**: 4016030, https://doi.org/10.1061/(ASCE)GM.1943-5622.0000666.

Wehnert M and Vermeer PA (2004) Numerical analyses of load tests on bored piles. In *Numerical Methods in Geomechanics: Proceedings of the 9th International Symposium on Numerical Models in Geomechanics – NUMOG IX, 25–27 August 2004, Ottawa, Canada* (Pande GN and Pietruszczak S (eds)). CRC Press/Balkema, Leiden, the Netherlands, pp. 505–511.

Yavari N, Tang AM, Pereira JM and Hassen G (2014) Experimental study on the mechanical behaviour of a heat exchanger pile using physical modelling. *Acta Geotechnica* **9(3)**: 385–398, https://doi.org/10.1007/s11440-014-0310-7.

Yavari N, Tang AM, Pereira JM and Hassen G (2016a) Mechanical behaviour of a small-scale energy pile in saturated clay. *Géotechnique* **66(11)**: 878–887, https://doi.org/10.1680/jgeot.15.T.026.

Yavari N, Tang AM, Pereira JM and Hassen G (2016b) Effect of temperature on the shear strength of soils and soil/structure interface. *Canadian Geotechnical Journal* **53(7)**: 1186–1194, https://doi.org/10.1139/cgj-2015-0355.

How can you contribute?

To discuss this paper, please submit up to 500 words to the editor at journals@ice.org.uk. Your contribution will be forwarded to the author(s) for a reply and, if considered appropriate by the editorial board, it will be published as a discussion in a future issue of the journal.

Author Queries

Q1: ‘energy pile’, ‘numerical modelling’, ‘physical modelling’, ‘saturated clay’, ‘thermal cycles’, and ‘thermo-mechanical behaviour’ are not valid keywords. Please select 3 keywords from the Environmental Geotechnics list (https://www.icevirtuallibrary.com/pb-assets/for%20authors/ENGE%20keywords%20November%202018-1542295903957.pdf).
Q2: Please provide full first names for authors Nguyen, Wu, Gan, and Pereira.
Q3: Please provide post-nominal qualifications and job titles for all authors.
Q4: Please check that the affiliation “Laboratoire Navier” is presented correctly.
Q5: Please check if “on an underground” can be changed to “below ground” for clarity.
Q6: Please check change to “into a layer of 50 mm thickness”.
Q7: Please define OCR.
Q8: Please verify that changes in the sentence "The former is calculated based on the Cam-clay ..." have preserved your meaning.
Q9: Please define CHS.
Q10: “Wehnert *et al*. (2004)” has been changed to “Wehnert and Vermeer (2004)” to match the entry in the reference list. Please check.
Q11: Please check change to “soil–pile interaction”.
Q12: Please define ANR.
Q13: Please provide DOI for Abuel-Naga H, Raouf MIN, Raouf AMI and Nasser AG (2015), Lv YR, Ng CWW, Lam SY, Liu HL and Ma LJ (2017), Nguyen VT, Tang AM and Pereira JM (2017), .
Q14: Pasten *et al*. (2013) is not cited in the text. Please insert a citation or delete the reference.